New applications of `carlomat`

Karol Kołodziej

Institute of Physics, University of Silesia

Katowice

Loops and Legs in Quantum Field Theory

Weimar, 27 April - 2 May, 2014

carlomat_v2.0

carlomat is a program for automatic computation of the lowest order cross sections of multiparticle reactions,

carlomat_v2.0

carlomat is a program for automatic computation of the lowest order cross sections of multiparticle reactions, dedicated mainly to description of the processes of production and decay of heavy particles such as, e.g., top quarks, Higgs boson, or electroweak gauge bosons.

carlomat_v2.0

carlomat is a program for automatic computation of the lowest order cross sections of multiparticle reactions, dedicated mainly to description of the processes of production and decay of heavy particles such as, e.g., top quarks, Higgs boson, or electroweak gauge bosons.

Substantial modifications with respect to version 1 of the program include:

carlomat_v2.0

carlomat is a program for automatic computation of the lowest order cross sections of multiparticle reactions, dedicated mainly to description of the processes of production and decay of heavy particles such as, e.g., top quarks, Higgs boson, or electroweak gauge bosons.

Substantial modifications with respect to version 1 of the program include:

- generation of a single phase space parameterization for the Feynman diagrams of the same topology,

carlomat_v2.0

`carlomat` is a program for automatic computation of the lowest order cross sections of multiparticle reactions, dedicated mainly to description of the processes of production and decay of heavy particles such as, e.g., top quarks, Higgs boson, or electroweak gauge bosons.

Substantial modifications with respect to version 1 of the program include:

- generation of a single phase space parameterization for the Feynman diagrams of the same topology,
- an interface to parton density functions,

carlomat_v2.0

carlomat is a program for automatic computation of the lowest order cross sections of multiparticle reactions, dedicated mainly to description of the processes of production and decay of heavy particles such as, e.g., top quarks, Higgs boson, or electroweak gauge bosons.

Substantial modifications with respect to version 1 of the program include:

- generation of a single phase space parameterization for the Feynman diagrams of the same topology,
- an interface to parton density functions,
- improvement of the color matrix computation,

carlomat_v2.0

- the Cabibbo-Kobayashi-Maskawa mixing in the quark sector,

carlomat_v2.0

- the Cabibbo-Kobayashi-Maskawa mixing in the quark sector,
- effective models, including scalar electrodynamics, the Wtb interaction with operators of dimension up to 5 and a general top-Higgs coupling.

carlomat_v2.0

- the Cabibbo-Kobayashi-Maskawa mixing in the quark sector,
- effective models, including scalar electrodynamics, the Wtb interaction with operators of dimension up to 5 and a general top-Higgs coupling.

Moreover, some minor modifications have been made and several bugs in the program have been corrected.

carlomat_v2.0

- the Cabibbo-Kobayashi-Maskawa mixing in the quark sector,
- effective models, including scalar electrodynamics, the Wtb interaction with operators of dimension up to 5 and a general top-Higgs coupling.

Moreover, some minor modifications have been made and several bugs in the program have been corrected.
Version 2 of `carlomat` was released in summer 2013 and the paper: KK, Comput. Phys. Commun. **185** (2014) 323, [arXiv:1305.5096],

was published in the beginning of 2014.

carlomat_v2.0

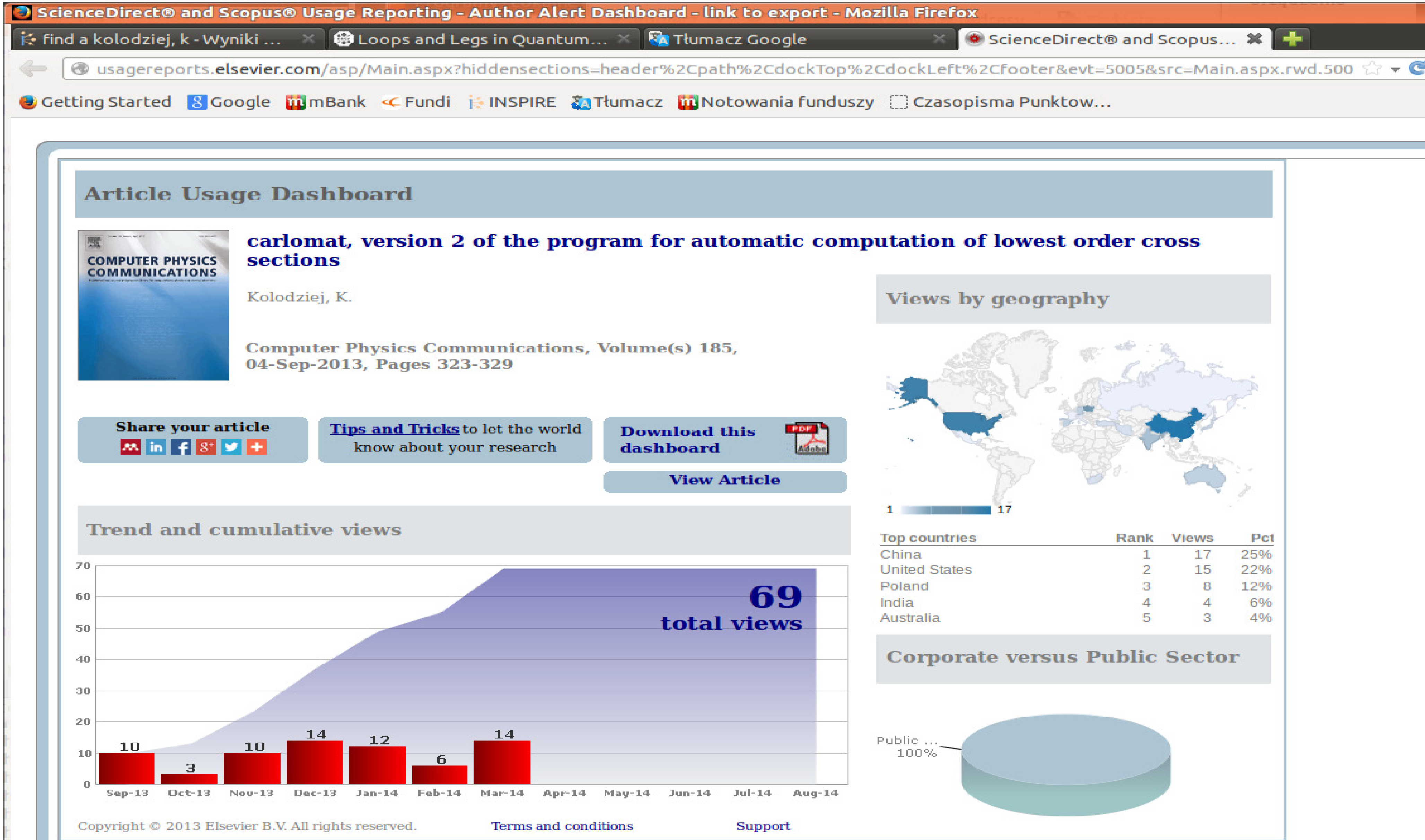

Phase space integration

The number of peaks in the squared matrix element usually by far exceeds the number of independent variables in a single parameterization of the phase space integration element.

Phase space integration

The number of peaks in the squared matrix element usually by far exceeds the number of independent variables in a single parameterization of the phase space integration element.

The phase space integration in `carlomat` is performed with the use of multichannel MC approach.

Phase space integration

The number of peaks in the squared matrix element usually by far exceeds the number of independent variables in a single parameterization of the phase space integration element.

The phase space integration in `carlomat` is performed with the use of multichannel MC approach.

In version 1 of the program, a separate phase space parameterization is generated for each Feynman diagram whose peaks are smoothed with appropriate mappings of the integration variables.

Phase space integration

The number of peaks in the squared matrix element usually by far exceeds the number of independent variables in a single parameterization of the phase space integration element.

The phase space integration in `carlomat` is performed with the use of multichannel MC approach.

In version 1 of the program, a separate phase space parameterization is generated for each Feynman diagram whose peaks are smoothed with appropriate mappings of the integration variables.

The parameterizations are automatically combined in a single multichannel phase space integration routine.

Phase space integration

However, the Feynman diagrams of the same topology differ from each other only in propagators of the internal particles.

Phase space integration

However, the Feynman diagrams of the same topology differ from each other only in propagators of the internal particles. The integration limits of all the variables and the Lorentz boosts of four momenta of the final state are the same for the diagrams of the same topology are common and can be written only once.

Phase space integration

However, the Feynman diagrams of the same topology differ from each other only in propagators of the internal particles. The integration limits of all the variables and the Lorentz boosts of four momenta of the final state are the same for the diagrams of the same topology are common and can be written only once.

The phase space integration routine in `carlomat_v2.0` becomes shorter and a compilation time is reduced, by a factor of 4–5 for multiparticle reactions, compared to the previous version of the program.

Hadron–hadron collisions and color matrix

Interfaces to `MSTW` and `CTEQ6` PDFs are added in the MC computation part of the program.

Hadron–hadron collisions and color matrix

Interfaces to `MSTW` and `CTEQ6` PDFs are added in the MC computation part of the program.

The user should choose if she/he wants to calculate the cross section of the hard scattering process at the fixed centre of mass energy, or to fold it with the parton density functions, treating the initial state particles as partons of either the $p\bar{p}$ or pp scattering.

Hadron–hadron collisions and color matrix

Interfaces to `MSTW` and `CTEQ6` PDFs are added in the MC computation part of the program.

The user should choose if she/he wants to calculate the cross section of the hard scattering process at the fixed centre of mass energy, or to fold it with the parton density functions, treating the initial state particles as partons of either the $p\bar{p}$ or pp scattering.

A subroutine `colsqkk` that computes the reduced color matrix is divided into smaller subroutines of the user controlled size which allows to compile much larger color matrices and speeds up the compilation process.

Hadron–hadron collisions and color matrix

Interfaces to `MSTW` and `CTEQ6` PDFs are added in the MC computation part of the program.

The user should choose if she/he wants to calculate the cross section of the hard scattering process at the fixed centre of mass energy, or to fold it with the parton density functions, treating the initial state particles as partons of either the $p\bar{p}$ or pp scattering.

A subroutine `colsqkk` that computes the reduced color matrix is divided into smaller subroutines of the user controlled size which allows to compile much larger color matrices and speeds up the compilation process.

Computation of the color matrix is performed as a separate stage, that is automatically executed just after the code generation and only the nonzero elements are transferred to the MC program.

Cabibbo-Kobayashi-Maskawa mixing

The CKM mixing in the quark sector is implemented in the program.

Cabibbo-Kobayashi-Maskawa mixing

The CKM mixing in the quark sector is implemented in the program.

As it would be an unnecessary complication for many applications, it can be switched on or off.

Cabibbo-Kobayashi-Maskawa mixing

The CKM mixing in the quark sector is implemented in the program.

As it would be an unnecessary complication for many applications, it can be switched on or off.

For the sake of simplicity, only the magnitudes of the CKM matrix elements V_{ij} are taken into account.

Cabibbo-Kobayashi-Maskawa mixing

The CKM mixing in the quark sector is implemented in the program.

As it would be an unnecessary complication for many applications, it can be switched on or off.

For the sake of simplicity, only the magnitudes of the CKM matrix elements V_{ij} are taken into account.

However, the complex phase of the CKM matrix can be easily incorporated, as the W boson coupling to fermions that always multiplies V_{ij} is complex.

Cabibbo-Kobayashi-Maskawa mixing

The CKM mixing in the quark sector is implemented in the program.

As it would be an unnecessary complication for many applications, it can be switched on or off.

For the sake of simplicity, only the magnitudes of the CKM matrix elements V_{ij} are taken into account.

However, the complex phase of the CKM matrix can be easily incorporated, as the W boson coupling to fermions that always multiplies V_{ij} is complex.

If the CKM mixing is included then the numbers Feynman diagrams of hadronic reactions grows substantially.

Anomalous Wtb coupling

The effective Lagrangian of the Wtb interaction containing operators of dimension four and five that is implemented in the current version of the program has the following form:

$$
\begin{aligned}
L_{Wtb} \;=\; & \frac{g}{\sqrt{2}} V_{tb} \left[W_\mu^- \bar{b} \gamma^\mu \left(f_1^L P_L + f_1^R P_R \right) t \right. \\
& \left. \qquad - \frac{1}{m_W} \partial_\nu W_\mu^- \bar{b} \sigma^{\mu\nu} \left(f_2^L P_L + f_2^R P_R \right) t \right] \\
+ \; & \frac{g}{\sqrt{2}} V_{tb}^* \left[W_\mu^+ \bar{t} \gamma^\mu \left(\bar{f}_1^L P_L + \bar{f}_1^R P_R \right) b \right. \\
& \left. \qquad - \frac{1}{m_W} \partial_\nu W_\mu^+ \bar{t} \sigma^{\mu\nu} \left(\bar{f}_2^L P_L + \bar{f}_2^R P_R \right) b \right],
\end{aligned}
$$

Anomalous Wtb coupling

The effective Lagrangian of the *Wtb* interaction containing operators of dimension four and five that is implemented in the current version of the program has the following form:

$$
\begin{aligned}
L_{Wtb} \;=\; & \frac{g}{\sqrt{2}} V_{tb} \left[W_\mu^- \bar{b} \gamma^\mu \left(f_1^L P_L + f_1^R P_R \right) t \right. \\
& \left. - \frac{1}{m_W} \partial_\nu W_\mu^- \bar{b} \sigma^{\mu\nu} \left(f_2^L P_L + f_2^R P_R \right) t \right] \\
+ \; & \frac{g}{\sqrt{2}} V_{tb}^* \left[W_\mu^+ \bar{t} \gamma^\mu \left(\bar{f}_1^L P_L + \bar{f}_1^R P_R \right) b \right. \\
& \left. - \frac{1}{m_W} \partial_\nu W_\mu^+ \bar{t} \sigma^{\mu\nu} \left(\bar{f}_2^L P_L + \bar{f}_2^R P_R \right) b \right],
\end{aligned}
$$

Couplings f_i^L, f_i^R, $\bar{f}_i^L$, $\bar{f}_i^R$, $i = 1, 2$, can be complex in general.

In the SM, $f_1^L = \bar{f}_1^L = 1$ and other couplings are 0.

Anomalous Wtb coupling

If CP is conserved then the following relationships hold:

$$\bar{f}_1^{R\,*} = f_1^R, \quad \bar{f}_1^{L\,*} = f_1^L, \qquad \bar{f}_2^{R\,*} = f_2^L, \quad \bar{f}_2^{L\,*} = f_2^R.$$

Anomalous Wtb coupling

If CP is conserved then the following relationships hold:

$$\bar{f}_1^{R\,*} = f_1^R, \quad \bar{f}_1^{L\,*} = f_1^L, \qquad \bar{f}_2^{R\,*} = f_2^L, \quad \bar{f}_2^{L\,*} = f_2^R.$$

The top quark width Γ_t is calculated anew, every time the form factors f_i^L, f_i^R, $\bar{f}_i^L$ and $\bar{f}_i^R$, $i = 1, 2$, are changed.

Anomalous Wtb coupling

If CP is conserved then the following relationships hold:

$$\bar{f}_1^{R\,*} = f_1^R, \quad \bar{f}_1^{L\,*} = f_1^L, \qquad \bar{f}_2^{R\,*} = f_2^L, \quad \bar{f}_2^{L\,*} = f_2^R.$$

The top quark width Γ_t is calculated anew, every time the form factors f_i^L, f_i^R, $\bar{f}_i^L$ and $\bar{f}_i^R$, $i = 1, 2$, are changed.

For CP-odd choices of the couplings, $\Gamma_t \neq \Gamma_{\bar{t}} \quad \Rightarrow$

Anomalous Wtb coupling

If CP is conserved then the following relationships hold:

$$\bar{f}_1^{R\,*} = f_1^R, \quad \bar{f}_1^{L\,*} = f_1^L, \qquad \bar{f}_2^{R\,*} = f_2^L, \quad \bar{f}_2^{L\,*} = f_2^R.$$

The top quark width Γ_t is calculated anew, every time the form factors f_i^L, f_i^R, $\bar{f}_i^L$ and $\bar{f}_i^R$, $i = 1, 2$, are changed.

For CP-odd choices of the couplings, $\Gamma_t \neq \Gamma_{\bar{t}} \quad \Rightarrow \quad$ both widths are calculated and the following rule is applied in the s-channel top quark propagators: Γ_t is used if the propagator goes into W^+b and $\Gamma_{\bar{t}}$ is used if the propagator goes into $W^-\bar{b}$.

Anomalous Wtb coupling

If CP is conserved then the following relationships hold:

$$\bar{f}_1^{R\,*} = f_1^R, \quad \bar{f}_1^{L\,*} = f_1^L, \qquad \bar{f}_2^{R\,*} = f_2^L, \quad \bar{f}_2^{L\,*} = f_2^R.$$

The top quark width Γ_t is calculated anew, every time the form factors f_i^L, f_i^R, $\bar{f}_i^L$ and $\bar{f}_i^R$, $i = 1, 2$, are changed.

For CP-odd choices of the couplings, $\Gamma_t \neq \Gamma_{\bar{t}} \quad \Rightarrow \quad$ both widths are calculated and the following rule is applied in the s-channel top quark propagators: Γ_t is used if the propagator goes into W^+b and $\Gamma_{\bar{t}}$ is used if the propagator goes into $W^-\bar{b}$.

The rule does not work for the propagators in t- or u-channels, but the actual value of the top quark width should not play much of a role in them.

Anomalous top–Higgs Yukawa coupling

The most general Lagrangian of $t\bar{t}h$ interaction including corrections from dimension-six operators that has been implemented in the program has the following form [J.A. Aguilar-Saavedra, NPB821 (2009) 215]:

$$\mathcal{L}_{t\bar{t}h} = -g_{t\bar{t}h}\bar{t}\left(f + if'\gamma_5\right)th,$$

f and f' that describe the scalar and pseudoscalar departures, respectively, from a purely scalar top–Higgs Yukawa coupling $g_{t\bar{t}h}$ of SM are assumed to be real.

The top–Higgs Yukawa coupling of SM is reproduced for $f = 1$ and $f' = 0$.

Associated $t\bar{t}H$ production at LHC

Examples of the Feynman diagrams of $gg \to bu\bar{d}\bar{b}\mu^-\bar{\nu}_\mu b\bar{b}$:

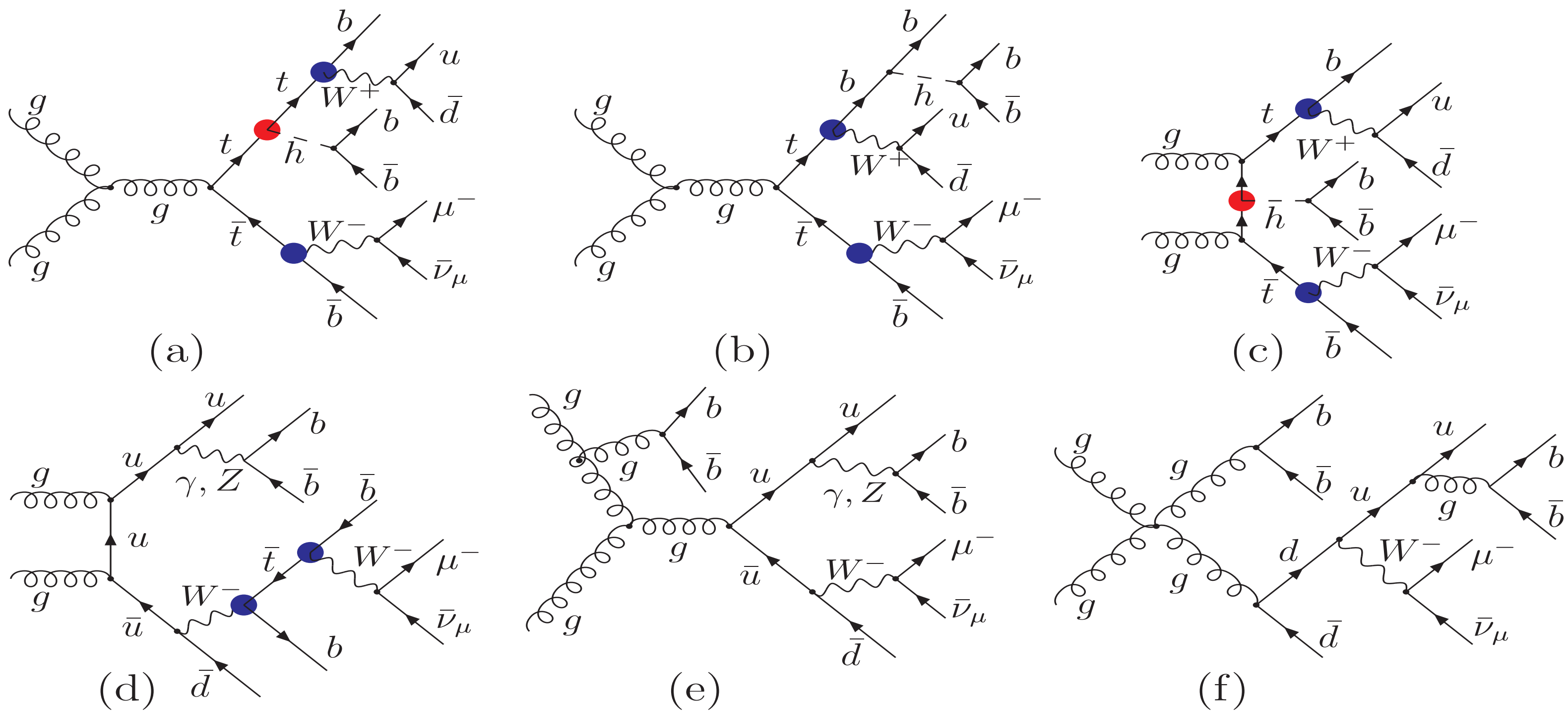

Red (blue) blobs indicate the top-Higgs (Wtb) coupling.

67 300 diagrams in the leading order of the SM, in the unitary gauge, neglecting masses smaller than m_b and the CKM mixing.

$pp \to b\bar{b}bu\bar{d}\bar{b}\mu^-\bar{\nu}_\mu$ at $\sqrt{s} = 14$ TeV

Distributions in cosine of the μ^--Higgs boson angle with signal (left) and all (right) Feynman diagrams (CTEQ6L PDFs with $Q = 2m_t + m_h$):

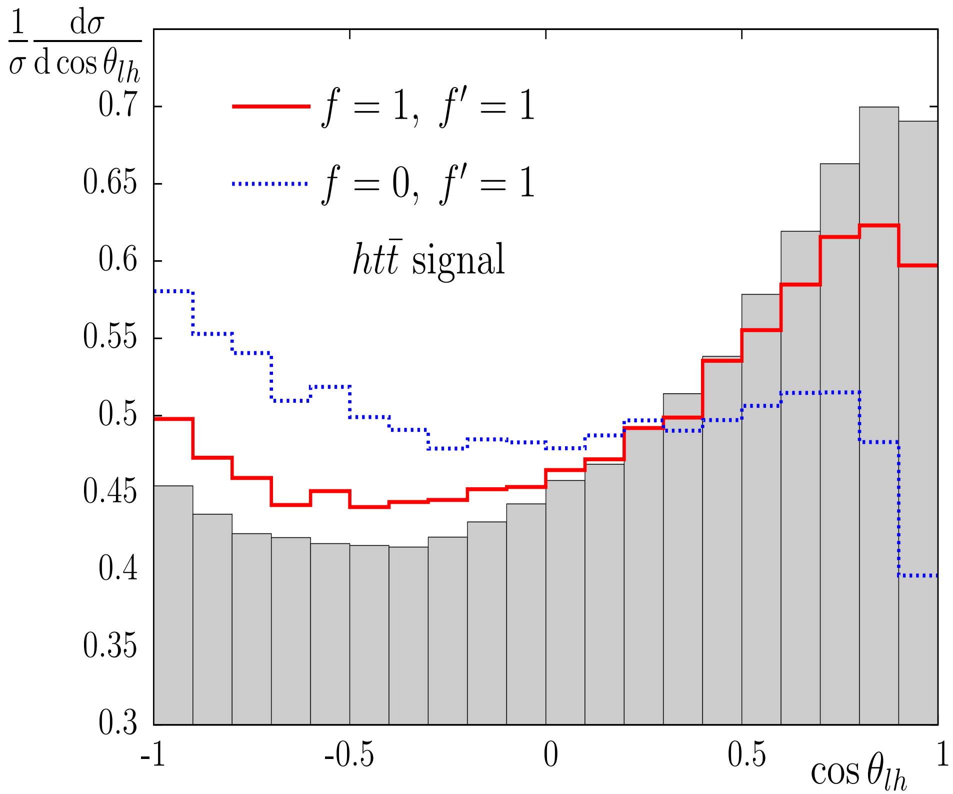

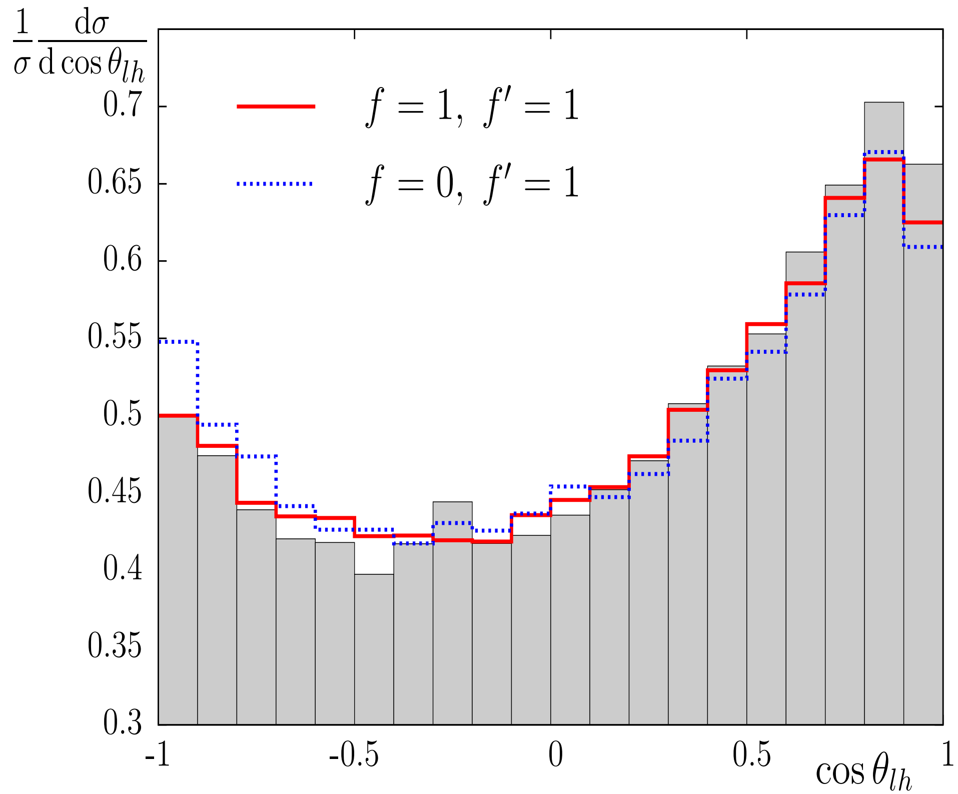

From KK, JHEP **07** (2013) 083.

$e^+e^- \to$ *hadrons at low energies*

The knowledge of $\sigma_{e^+e^-\to\mathrm{hadrons}}(s)$ allows, through dispersion relations, for determination of hadronic contributions to the vacuum polarization.

$e^+e^- \to$ *hadrons at low energies*

The knowledge of $\sigma_{e^+e^- \to \text{hadrons}}(s)$ allows, through dispersion relations, for determination of hadronic contributions to the vacuum polarization.

$\Rightarrow$ Better precision of theoretical predictions for the muon anomalous magnetic moment and evolution of the fine structure constant from the Thomson limit to high energy scales.

$e^+e^- \to$ *hadrons at low energies*

The knowledge of $\sigma_{e^+e^-\to \mathrm{hadrons}}(s)$ allows, through dispersion relations, for determination of hadronic contributions to the vacuum polarization.

$\Rightarrow$ Better precision of theoretical predictions for the muon anomalous magnetic moment and evolution of the fine structure constant from the Thomson limit to high energy scales.

Below the J/ψ threshold, $\sigma_{e^+e^-\to \mathrm{hadrons}}(s)$ must be measured, either by the initial beam energy scan or with the use of a radiative return method.

$e^+e^- \to$ *hadrons at low energies*

The knowledge of $\sigma_{e^+e^-\to\text{hadrons}}(s)$ allows, through dispersion relations, for determination of hadronic contributions to the vacuum polarization.

$\Rightarrow$ Better precision of theoretical predictions for the muon anomalous magnetic moment and evolution of the fine structure constant from the Thomson limit to high energy scales.

Below the J/ψ threshold, $\sigma_{e^+e^-\to\text{hadrons}}(s)$ must be measured, either by the initial beam energy scan or with the use of a radiative return method.

At low energies, the hadronic final states consist mostly of pions, accompanied by one or more photons.

Scalar electrodynamics (sQED)

sQED allows to describe effectively the low energetic EM interaction of charged pions.

Scalar electrodynamics (sQED)

sQED allows to describe effectively the low energetic EM interaction of charged pions. At low energies, $\pi^{\pm}$ can be treated as point like particles represented by a complex scalar field φ.

Scalar electrodynamics (sQED)

sQED allows to describe effectively the low energetic EM interaction of charged pions. At low energies, $\pi^{\pm}$ can be treated as point like particles represented by a complex scalar field φ. The $U(1)$ gauge invariant Lagrangian of sQED implemented in `carlomat` has the form:

$$\begin{aligned}\mathcal{L}_{\pi}^{\mathrm{sQED}} &= \partial_{\mu}\varphi\,(\partial^{\mu}\varphi)^{*} - m_{\pi}^{2}\varphi\varphi^{*} - ie\left(\varphi^{*}\partial_{\mu}\varphi - \varphi\partial_{\mu}\varphi^{*}\right)A^{\mu} \\ &\quad + e^{2}g_{\mu\nu}\varphi\varphi^{*}A^{\mu}A^{\nu}.\end{aligned}$$

Scalar electrodynamics (sQED)

sQED allows to describe effectively the low energetic EM interaction of charged pions. At low energies, $\pi^{\pm}$ can be treated as point like particles represented by a complex scalar field φ. The $U(1)$ gauge invariant Lagrangian of sQED implemented in `carlomat` has the form:

$$\begin{aligned} \mathcal{L}_{\pi}^{\mathrm{sQED}} &= \partial_{\mu}\varphi\left(\partial^{\mu}\varphi\right)^{*} - m_{\pi}^{2}\varphi\varphi^{*} - ie\left(\varphi^{*}\partial_{\mu}\varphi - \varphi\partial_{\mu}\varphi^{*}\right)A^{\mu} \\ &\qquad + e^{2}g_{\mu\nu}\varphi\varphi^{*}A^{\mu}A^{\nu}. \end{aligned}$$

The bound state nature of the charged pion can be taken into account by the substitutions:

$$e \to eF_{\pi}(q^{2}), \qquad e^{2} \to e^{2}\left|F_{\pi}(q^{2})\right|^{2},$$

where $F_{\pi}(q^{2})$ is the charged pion form factor (not implemented).

Recent developments in `carlomat`

The EM current of spin 1/2 nucleons that was recently implemented in `carlomat` has the form:

$$J^\mu = e\bar{N}(p')\left[\gamma^\mu F_1(Q^2) + \frac{i}{2m_N}\sigma^{\mu\nu} q_\nu F_2(Q^2)\right] N(p),$$

similar to the form of the Wtb interaction vertex in L_{Wtb}.

Recent developments in `carlomat`

The EM current of spin 1/2 nucleons that was recently implemented in `carlomat` has the form:

$$J^\mu \;=\; e\bar{N}(p')\left[\gamma^\mu F_1(Q^2) + \frac{i}{2m_N}\sigma^{\mu\nu}q_\nu F_2(Q^2)\right]N(p),$$

similar to the form of the Wtb interaction vertex in L_{Wtb}. Form factors $F_1(Q^2)$ and $F_2(Q^2)$, where $Q^2 = -q^2$, have been adopted from PHOKARA.

Recent developments in `carlomat`

The EM current of spin 1/2 nucleons that was recently implemented in `carlomat` has the form:

$$J^\mu = e\bar{N}(p')\left[\gamma^\mu F_1(Q^2) + \frac{i}{2m_N}\sigma^{\mu\nu} q_\nu F_2(Q^2)\right] N(p),$$

similar to the form of the Wtb interaction vertex in L_{Wtb}.
Form factors $F_1(Q^2)$ and $F_2(Q^2)$, where $Q^2 = -q^2$, have been adopted from PHOKARA.

Simulation of processes involving the EM interaction of nucleons.

Recent developments in `carlomat`

Work on implementation of the Feynman rules of the Resonance Chiral Perturbation Theory provided by Fred Jegerlehner is ongoing.

Recent developments in `carlomat`

Work on implementation of the Feynman rules of the Resonance Chiral Perturbation Theory provided by Fred Jegerlehner is ongoing.

Implementation of new triple and quartic vertices is straightforward.

Recent developments in `carlomat`

Work on implementation of the Feynman rules of the Resonance Chiral Perturbation Theory provided by Fred Jegerlehner is ongoing.

Implementation of new triple and quartic vertices is straightforward.

Implementation of the particle mixing is more challenging.

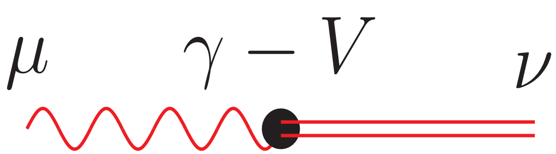

$$\equiv \; -e f_{\gamma V} \, g^{\mu\nu}$$

Substantial changes in the code generating part of the program are required.

Recent developments in `carlomat`

Topologies are generated for models with triple and quartic couplings, starting with 1 topology of a 3 particle process.

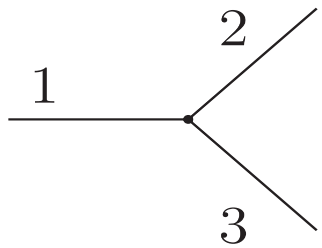

Recent developments in `carlomat`

Topologies are generated for models with triple and quartic couplings, starting with 1 topology of a 3 particle process.

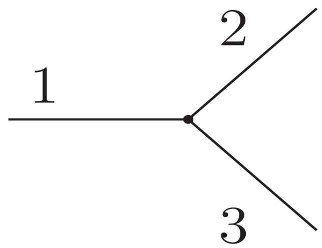

Line 4 is attached to each line and to the vertex $\Rightarrow$ 4 topologies of a 4 particle process.

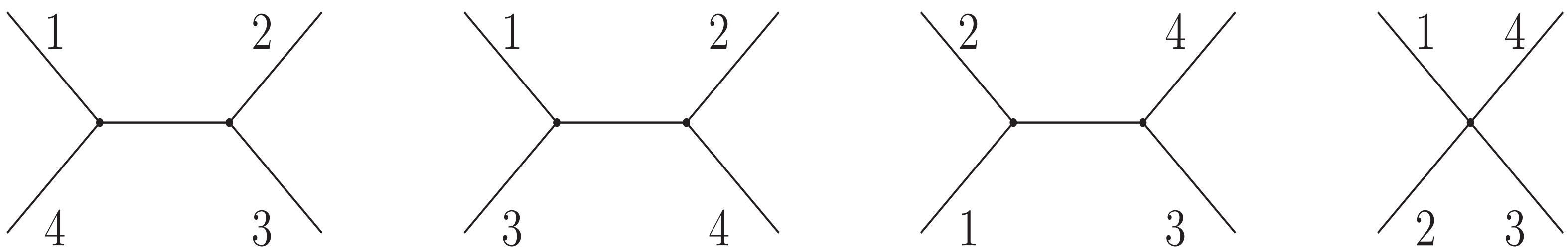

Recent developments in `carlomat`

Topologies are generated for models with triple and quartic couplings, starting with 1 topology of a 3 particle process.

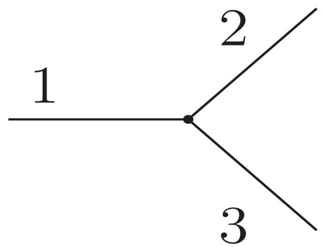

Line 4 is attached to each line and to the vertex $\Rightarrow$ 4 topologies of a 4 particle process.

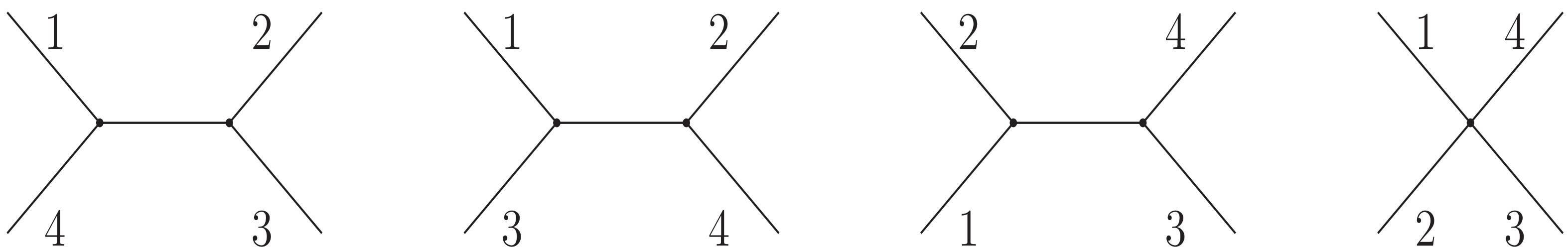

Line 5 is attached to each line, including the internal ones, and to each triple vertex $\Rightarrow$ 25 topologies of a 5 particle process.

Recent developments in `carlomat`

No. of topologies grows dramatically with No. of external particles.

No. of particles	No. of topologies
6	220
7	2 485
8	34 300
9	559 405
10	10 525 900
11	224 449 225

Recent developments in `carlomat`

No. of topologies grows dramatically with No. of external particles.

No. of particles	No. of topologies
6	220
7	2 485
8	34 300
9	559 405
10	10 525 900
11	224 449 225

n external particles $\Rightarrow$ topologies for $n-1$ particles needed

Recent developments in `carlomat`

No. of topologies grows dramatically with No. of external particles.

No. of particles	No. of topologies
6	220
7	2 485
8	34 300
9	559 405
10	10 525 900
11	224 449 225

n external particles $\Rightarrow$ topologies for $n-1$ particles needed

$\Rightarrow$ Feynman rules checked while adding the n-th particle.

Recent developments in `carlomat`

No. of topologies grows dramatically with No. of external particles.

No. of particles	No. of topologies
6	220
7	2 485
8	34 300
9	559 405
10	10 525 900
11	224 449 225

n external particles $\Rightarrow$ topologies for $n-1$ particles needed

$\Rightarrow$ Feynman rules checked while adding the n-th particle.

The particle mixing is added just at this stage.

Thank you for your attention